Journal of Chromatography A, 1216 (2009) 7360–7367

Contents lists available at ScienceDirect

Journal of Chromatography A

journal homepage: www.elsevier.com/locate/chroma

Effect of the presence of an ordered micro-pillar array on the formation of silica monoliths

Frederik Detobel[a], Hamed Eghbali[a], Selm De Bruyne[a], Herman Terryn[b], Han Gardeniers[c], Gert Desmet[a,*]

[a] Vrije Universiteit Brussel, Department of Chemical Engineering, Pleinlaan 2, 1050 Brussels, Belgium
[b] Vrije Universiteit Brussel, Department of Materials and Chemistry, Pleinlaan 2, 1050 Brussels, Belgium
[c] Research Program Mesofluidics, MESA+ Institute for Nanotechnology, De Veldmaat 10, 7522 NM Enschede, The Netherlands

ARTICLE INFO

Article history:
Available online 13 March 2009

Keywords:
Confined geometry
Micro-pillar array
Phase separation
Sol–gel
Chromatography
Wetting

ABSTRACT

We report on the synthesis of siloxane-based monoliths in the presence of a two-dimensional, perfectly ordered array of micro-pillars. Both methyltrimethoxysilane- and tetramethoxysilane-based monoliths were considered. The obtained structures were analyzed using scanning-electron microscopy and can be explained from the general theory of surface-directed phase separation in confined spaces. The formed structures are to a large extent nearly exclusively determined by the ratio between the bulk domain size of the monolith on the one hand and the distance between the micro-pillars on the other hand. When this ratio is small, the presence of the pillars has nearly no effect on the morphology of the produced monoliths. However, when the ratio approaches unity and ascends above it, some new types of monolith morphologies are induced, two of which appear to have interesting properties for use as novel chromatographic supports. One of these structures (obtained when the domain size/inter-pillar distance ratio is around unity) is a 3D network of linear interconnections between the pillars, organized such that all skeleton branches are oriented perpendicular to the micro-pillar surface. A second interesting structure is obtained at even higher values of the domain size/inter-pillar distance ratio. In this case, each individual micro-pillar is uniformly coated with a mesoporous shell.

1. Introduction

1.1. General introduction

During the last decade, some new stationary phase supports were introduced in the field of chromatography, driven by the ever increasing performance demands, especially for pharmaceutical and bio-analytical applications. One such a support is the silica monolith [1–4]. Unlike what is possible in packed bed columns, the pore size in this packing material can be tuned independently from the skeleton size, hence enabling the formation of a highly permeable structure while retaining a relatively small band broadening. Because of this increased permeability, long columns can be used without the generation of an excessive pressure drop. Hence, high plate numbers and a high peak capacity can be attained without the need of expensive ultra high pressure equipment [5]. The current generation of silica monoliths is however unable to compete with silica particle packed bed columns when fast separations with a limited number of plates are needed. These separations would require monoliths with domain sizes that are smaller than currently available. Attempts to further reduce the domain size of silica monoliths however also always inevitably leads to structures that are more heterogeneous, hence compromising their chromatographic performance. As shown theoretically in [6,7], there might even be a fundamental down limit below which the domain size cannot be reduced without running in an adverse effect of the domain size on the band broadening. Recently, Hara et al. made some important improvements on the homogeneity of these small domain monoliths [8]. The pursuit of highly ordered, small-domain monoliths is an important endeavor [9], because theoretical studies have shown that if such silica monoliths could be made, they would be able to outperform the particle bed column over the entire range of required plate numbers [10].

Another novel chromatographic support, intrinsically always perfectly ordered, is the micro-pillar column, fabricated in silicon or glass wafers using semiconductor etching technology. This concept was originally proposed by Regnier and co-workers in 1998 [11–13], and the improved chromatographic performance of this type of support has meanwhile been clearly demonstrated, both theoretically [14–16] and experimentally [17–20]. However, because of the low phase ratio (the micro-pillars are usually non-porous), micro-

* Corresponding author. Tel.: +32 2 629 32 51; fax: +32 2 629 32 48.
E-mail address: gedesmet@vub.ac.be (G. Desmet).

0021-9673/$ – see front matter © 2009 Elsevier B.V. All rights reserved.
doi:10.1016/j.chroma.2009.03.010

pillar array columns still suffer from a limited mass loadability and retentive capacity. Recently, a number of approaches were presented to improve the phase ratio of micro-pillar array columns. De Malsche et al. created a mesoporous shell micro-pillar array column by electrochemical anodization of the micro-pillar surface [21,22]. The resulting column exhibited a good retentive capacity but the minimal micro-pillar diameter is limited to 5 μm because of mechanical stability problems. Another way to improve the surface area was presented by Fonverne et al. [23]. They deposited a layer of carbon nanotubes on the surface of the microstructures to increase the surface area. The application field of this type of stationary phase is however very limited and the retention mechanism is still not fully understood. Another drawback of both approaches is the asymmetric location of the mesoporous layer in the chromatographic channel (i.e., the pillar surface and bottom surface have an increased phase ratio by the presence of a porous layer, while the top surface remains untreated). This asymmetry is expected to limit the chromatographic performance by additional band broadening effects [21].

Given the shortcomings of both the monolithic column and the pillar array column, the aim of the present work is to investigate the possibility of merging the sol–gel technology of silica monoliths with the micro-pillar array column technology, hoping to obtain a hybrid chromatographic support which exhibits a high degree of spatial order, combined with a well tunable phase ratio and structure. Therefore, several silica monoliths were fabricated inside micro-channels with an ordered array of micro-pillars and the influence of the presence of these pillars on the monolithic structure was evaluated based on scanning electron microscopy images. Both methyltrimethoxysilane and tetramethoxysilane-based monoliths were considered, as these are the monomers which are generally used for silica monolith synthesis.

1.2. Existing knowledge of monolith synthesis in bulk and in confined spaces

There are several publications that review the different silica monolith synthesis techniques [24–27]. For the present work, only the literature on the synthesis of silica monoliths via the sol–gel process using silicon alkoxides is relevant. In short, the synthesis of this type of silica monoliths is achieved by a concurrence of phase separation and sol–gel transition [26]. The starting materials are silicon alkoxides which are fully hydrolysed by adding a sufficient amount of water. Subsequently, siloxane oligomers are formed by polycondensation reactions and, depending on the nature of the silicon alkoxide and the additives used, a phase separation can be established between the solvent phase and an oligomer rich phase. This phase separation is preferentially spinodal, leading to a bicontinuous structure, which coarsens in time to reduce the interfacial energy between both phases and eventually would lead to a break up into fragmented structures. The latter is however countered by the fact that, throughout the process of phase separation, the continuous proceeding of polymerization reactions between the siloxane oligomers results in an increase of the phase viscosity. At a certain moment, denoted as the sol–gel transition point, a single connection across the entire system dimension is formed, which is strengthened in time by additional poly-condensation reactions (a process called “aging”). This sol–gel transition fixes the phase separation in one of its transient unstable configurations and enables the formation of a sponge-like silica monolithic structure after evaporation of the solvent-rich phase. By a manipulation of the time (gelation time) between the onset of phase-separation and the sol–gel transition point through a change in temperature, pH or amount of certain additives (porogens), structures with a different through-pore and skeleton size can be obtained.

However, when silica monolithic structures are fabricated in confined spaces, such as capillaries or micro-channels, the presence of wall surfaces can have a major influence on the monolithic structure [28–32]. During phase separation, a process called “surface-directed spinodal decomposition” occurs [33,34], whereby one of the two phases preferentially wets the surfaces of the container. This process is initially driven by the diffusion of molecules towards the surface. In this stage, a configuration is established whereby the surface is completely covered by the wetting layer to which the bicontinuous part above the surface is connected. The preferential wetting then induces a pressure gradient from the bicontinuous part to the wetting layer and, as the phase separation proceeds, more of the wettable phase is transferred from the bi-continuous part towards the surface wetting layer (hydrodynamic pumping). This hydrodynamic pumping is accompanied by a change in configuration of the bi-continuous structure whereby the surface region is depleted from the wettable phase and tubes are formed through which the phase is transported towards the surface. The longer the time between the phase separation and the sol–gel transition, the further the effect of the hydrodynamic pumping on the monolithic structure will reach and eventually, depending on the dimension of the confined space, a thick wetting layer is formed on the wall surface instead of a monolithic skeleton structure (a process denoted as “wetting transition” [30]).

2. Materials and methods

2.1. Micro-channel fabrication

The procedure for the fabrication of microfluidic channels with an ordered array of micro-pillars is similar as described elsewhere [19]. The pillar channels were defined in a silicon–glass sandwich. First, a 100 mm diameter silicon wafer (p-type, 5–10 cm resistivity) was thermally (dry) oxidized at 1100 °C until 700 nm silicon oxide was formed (Amtech Tempress Omega Junior, Tempress Systems B.V., Vaassen, The Netherlands). Then normal UV photolithography (photoresist: Olin 907-12) was used to define the pillar array column. Subsequently, the exposed silicon oxide was dry etched (Adixen AMS100DE, Alcatel Vacuum Technology, Culemborg, The Netherlands), leaving a patterned silicon oxide layer, which serves as a mask for a second lithographic step. In this step, the exposed silicon was etched with a Bosch-type deep reactive ion etch (Adixen AMS100SE, Alcatel Vacuum Technology, Culemborg, The Netherlands), leaving pillars of 20–25 μm height. Then, the remaining resist was removed by an oxygen plasma and nitric acid. Through-holes, necessary for liquid handling in the micro-channel were defined by photolithography on a dry resist foil (Ordyl BF410, Tokyo Oga Kogyo, Kanagawa, Japan). The exposed glass was subsequently powder blasted using 30 μm alumina particles. To remove the fluorocarbons, the wafers were set in a (wet) oxide furnace (Amtech Tempress Omega Junior) at 700 °C for 15 min, after which the wafers were cleaned in nitric acid and dipped in hydrofluoric acid (1% in H_2O). Subsequently, the wafers were wet oxidized again for 15 min in order to provide a maximum amount of silanol groups to ensure a good chemical bonding of the siloxane-based gels (see below). The top of the channels was formed by a 100 mm diameter Pyrex wafer (thickness 0.5 mm), anodically bonded to the silicon wafer (voltage ramped to a maximum of 1000 V at 400 °C on an EVG EV-501 wafer bonder (EV Group Inc., Schaerding, Austria)).

The rectangular microfluidic channels used in this work were 30 mm in length, 500 μm wide and about 20–25 μm in depth. The micro-pillar array consists of cylindrical micro-pillars with a diameter of 2.4 μm, arranged according to a perfectly ordered equilateral triangular grid as visualized in Fig. 1. Three types of grids were considered, each type having a different inter-pillar distance (fur-

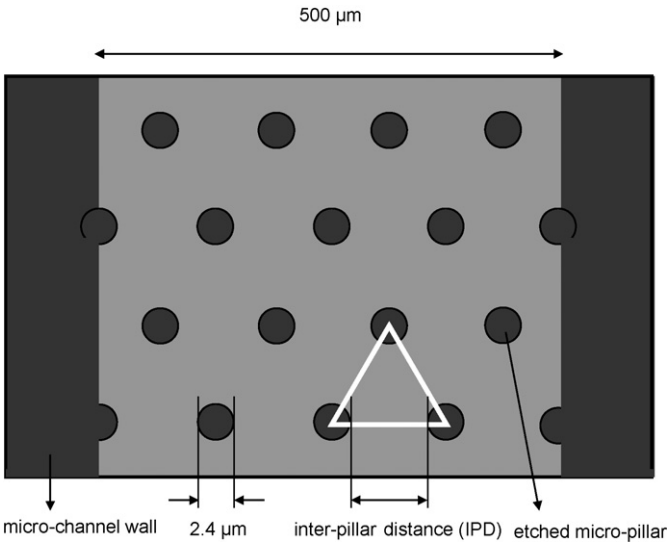

Fig. 1. Schematic representation of the pillar arrangement in a micro-pillar array column (not scaled).

ther denoted as IPD), respectively corresponding to 7.6, 5.6 and 3.6 μm.

2.2. Monolith synthesis

Two types of siloxane were used as monomers for the monolith synthesis: methyltrimethoxysilane (MTMS) and tetramethoxysilane (TMOS) (Sigma–Aldrich Inc., St. Louis, MO, USA).

The polymerization solution for the MTMS-based monoliths was prepared by homogeneously mixing 2.53 ml of a 1 M aqueous nitric acid (NA) solution (prepared inside a 20 ml glass vial) with an appropriate amount (further specified in Table 1) of methanol (MeOH) (Sigma–Aldrich Inc., St. Louis, MO, USA). Subsequently, 10 ml of MTMS was added to the solution and the mixture was stirred for 5 min at 0 °C.

In case of the TMOS-based monoliths, an appropriate amount (further specified in Table 2) of poly(ethyleneglycol) or PEG (Mw. 10,000, Sigma–Aldrich Inc., St. Louis, MO, USA) was dissolved in 10 ml of a 0.01 M aqueous acetic acid (AA) solution. Then, 4.5 ml of TMOS was added to the mixture and the solution was stirred for 45 min at 0 °C.

The phase separation and sol–gel reaction of both types of polymerization solutions was performed inside the microfluidic channels. For this purpose, the microfluidic chip was first placed in an in-house built PMMA holder. This holder allows to connect fused-silica capillary tubes to the in- and outlet holes of the chip by means of NanoPort assemblies (Upchurch Scientific Inc., Oak Harbor, WA, USA). The channels were subsequently filled with the polymerization solution using a syringe pump (KDS-220, KD-scientific Inc., Holliston, MA, USA) with disposable plastic syringes (Terumo Europe NV, Leuven, Belgium) connected to the capillary connection tubes. Then, the channel in- and outlets were closed and the gelation and aging of the polymerization solution was performed in the oven at 40 °C for 24 h. The gel was subsequently dried by opening the channel in- and outlets and leaving the chip for another 24 h at 40 °C. To be able to compare the structure of the monolith inside the micro-channels with the corresponding monolithic structure that could be obtained in the absence of a nearby surface, a bulk monolith was made inside a large glass vial (total volume of 20 ml and a diameter of 1 cm), starting from the same polymerization solution and using the same polymerization protocol.

2.3. Structure evaluation

The structure of the monoliths in bulk and inside the microfluidic channels was evaluated based on images taken by scanning electron microscopy (SEM) (Jeol JSM6400, Jeol Ltd., Tokyo, Japan) at an acceleration voltage of 20 kV and using a 3500× magnification. To improve the conductivity of the monolithic structures, a thin carbon coating was deposited on top of the sample. The average domain size of the silica monolith in bulk was estimated from these SEM images, using the image analysis software Vision Assistant 7.1 (National Instruments Belgium NV, Zaventem, Belgium).

3. Results and discussion

3.1. Initial experiments in cylindrical capillaries

To benchmark our procedures, we first synthesized a series of MTMS-based silica gels with different domain sizes in the 1D confined space of a cylindrical fused-silica capillary (with an internal diameter of 150 μm). Fig. 2 shows a sequence of SEM-images of the resulting structures. The structure in Fig. 2a is obtained with a low fraction of MeOH (which acts as a porogen). Under these conditions, the phase separation is arrested by the sol–gel transition in an early stage, yielding a monolithic structure with a small domain size. This monolithic structure is not influenced by the capillary surface. When the amount of methanol is increased, the onset of phase separation is accelerated and the sol–gel transition point is delayed by dilution effects. Consequently, the total period for phase separation becomes longer, hence coarsening the monolithic structure. With these increased amounts of MeOH, the effects of surface directed spinodal decomposition in the confined space of the capillary become apparent. First, a slight depletion of gel material can be observed along the capillary surface (Fig. 2b), but when the phase separation is allowed to proceed further, the hydrodynamic pump-

Table 1
Composition details and accompanying structural data for three different MTMS-based silica monoliths synthesized using different amounts of MeOH.

Composition name	1 M NA (ml)	MeOH (ml)	MTMS (ml)	Molar ratio (MTMS:MeOH:H_2O)	Pore size (μm)	Skeleton size (μm)	Domain size (μm)
M1	2.53	2.83	10	1:1.0:2	0.6	0.2	0.8
M2	2.53	3.26	10	1:1.15:2	2.6	0.6	3.2
M3	2.53	3.40	10	1:1.2:2	5.3	1.7	7.0

Table 2
Composition details and accompanying structural data for three different TMOS-based silica monoliths synthesized using different amounts of PEG.

Composition name	0.01 M AA (ml)	PEG (g)	TMOS (ml)	Molar ratio (TMOS:PEG:H_2O)	Pore size (μm)	Skeleton size (μm)	Domain size (μm)
T1	10	1.20	4	$1{:}4.9\times10^{-3}{:}20.43$	1.5	1.2	2.7
T2	10	1.00	4	$1{:}4.1\times10^{-3}{:}20.43$	3.4	2.1	5.5
T3	10	0.60	4	$1{:}2.5\times10^{-3}{:}20.43$	5.0	3.3	8.3

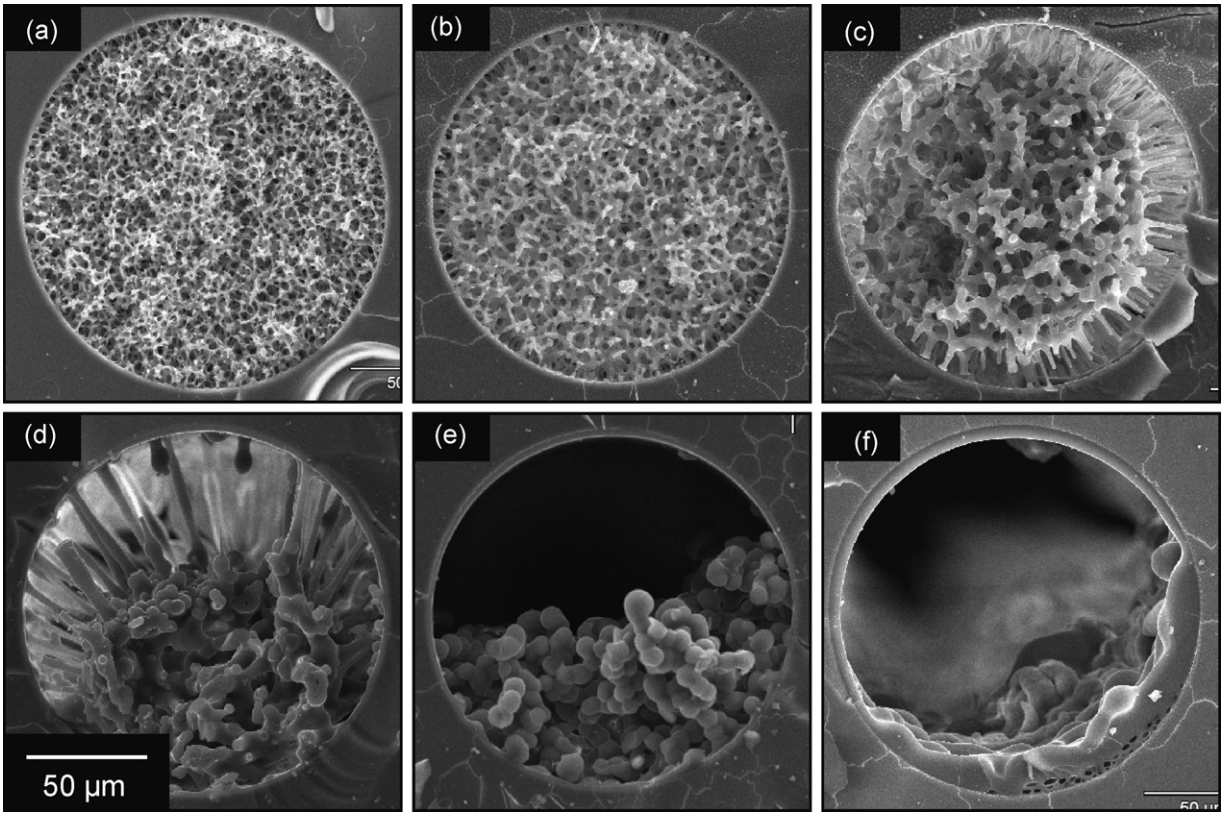

Fig. 2. SEM-images of MTMS-based monolithic structures inside a fused-silica capillary (internal diameter of 150 μm) arranged according to an increasing amount of porogen (MeOH). The molar ratios of MTMS:MeOH:H_2O are (a) 1:1.3:2, (b) 1:1.35:2, (c) 1:1.4:2, (d) 1:1.5:2, (e) 1:1.6:2 and (f) 1:1.8:2.

ing of gel material from the bicontinuous part towards the surface deforms an ever increasing part of the structure above the surface (Fig. 2c–e) until only a wetting layer, slightly deformed by gravity effects, remains on the capillary surface (Fig. 2f). These observations are in full agreement with the surface directed spinodal decomposition mechanisms described in the introduction (Section 1.2) and are also in line with previously reported results by Kanamori et al. [30]. They synthesized silica monoliths with a fixed composition in fused-silica capillaries with different diameters, while in the present study, different silica monolithic compositions (leading to different domain sizes) are tested inside fused-silica capillaries with a fixed diameter. The analogy between the observations made in both studies confirms that it is indeed the ratio between the domain size of the monolith and the dimension of the confined space that determines the outcome of the surface directed monolithic structure rather than their absolute value (as stated in [30]).

3.2. MTMS-based monolith synthesis in a micro-pillar array column

The first column of SEM-images in Fig. 3 shows some of the bulk monoliths obtained with different fractions of porogen (MeOH). As can be noted from the first column of SEM-images (Fig. 3a), an increment of the amount of porogen (corresponding to a transition from case i to case iii) is accompanied by a growth of the domain size (DS) of the monolith which can be explained by the differences in time between the onset of phase separation and the sol–gel transition (as described in Section 1.2). The 2nd, 3th and 4th column of SEM pictures in Fig. 3 show the corresponding structures obtained in pillar array channels with different inter-pillar distances (IPD), respectively 7.6, 5.6 and 3.6 μm. In the first row of Fig. 3(row i), the domain size of the monolith in bulk is all cases very small compared to all the inter-pillar distances (DS/IPD $\ll 1$) and the presence of the pillars inside the channels has no visible effect on the monolithic structure when compared to the monolithic structure in bulk. This can be understood from the fact that, in order to obtain such a small domain size, the phase separation is arrested by the sol–gel transition in an early stage. In this stage, the wetting of the surface is still mainly diffusion driven and the hydrodynamic pumping of the silica gel from the bi-continuous region towards the surface is largely prevented by the early sol–gel transition, hence yielding a structure which is not markedly influenced by the presence of micro-pillars. When the time between the onset of phase separation and sol–gel transition is increased, a monolith with a larger domain size is obtained. This is the case for the conditions shown in Fig. 3row ii. During this prolonged phase separation, the gel phase is able to wet the pillar surfaces by hydrodynamic pumping, hence deforming the monolithic structure near the pillar surface. In Fig. 3ii-b and -c, the inter-pillar distance is only slightly larger than the domain size of the monolith (DS/IPD < 1) and the effect of surface directed spinodal decomposition is visible throughout the whole monolithic structure, as only structures remain which form interconnections between the pillars. As seen in Fig. 3ii-d, the orientation of these interconnections becomes more uniform when the domain size of the monolith becomes of about the same size as the inter-pillar distance (DS/IPD$\sim$1). In this case, the pillars are strongly wetted with the gel phase and linear interconnections between the pillars, perpendicular to the pillar direction, are formed, yielding an apparently more homogeneous monolithic structure. Subsequently considering the third row of Fig. 3, similar effects can be observed. In Fig. 3iii-b, the domain size of the monolith is again of about the same size as the inter-pillar distance (conditions similar to those already encountered in Fig. 3ii-d). And again this leads to the formation of uniformly directed interconnections between the pillars, perpendicular to the pillar axis. The number of interconnections decreases

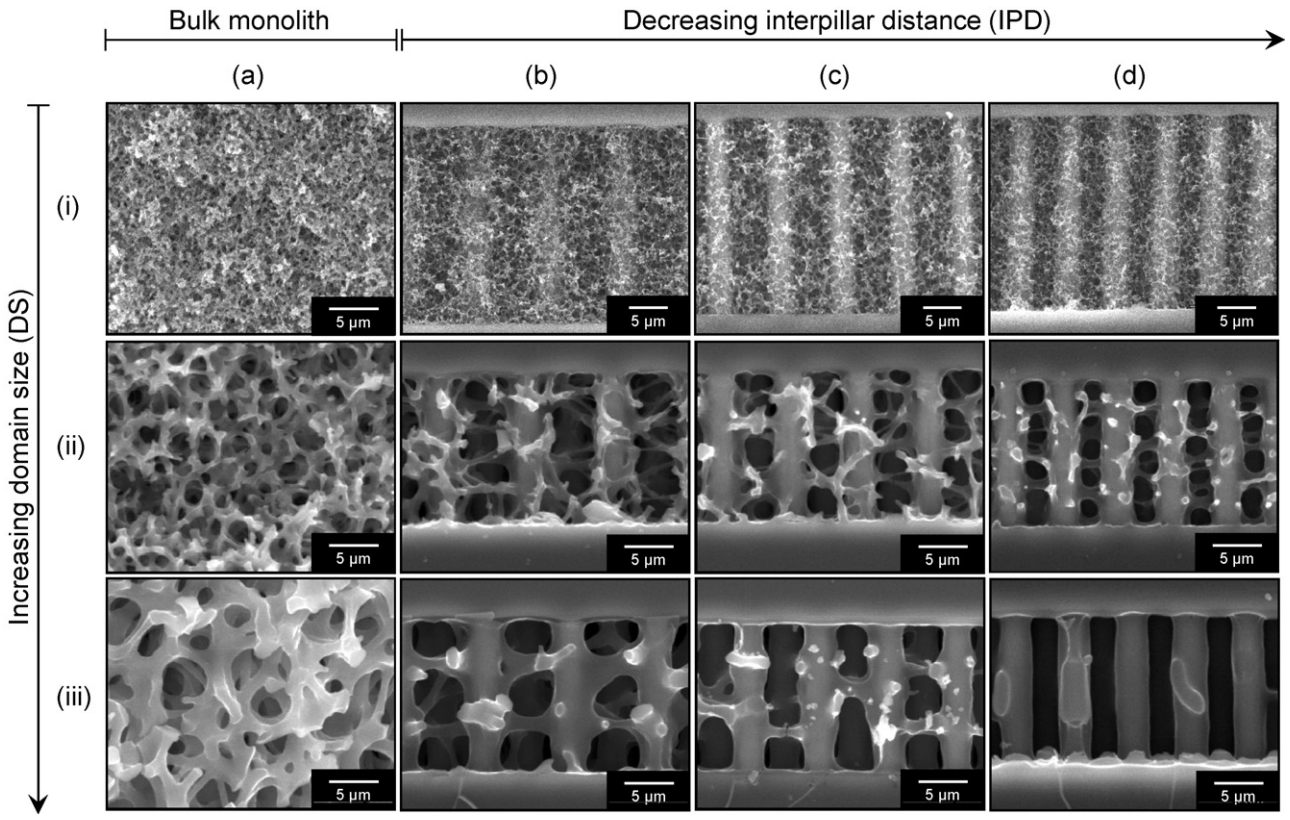

Fig. 3. SEM-images of MTMS-based gel structures, derived from three different compositions: (i) M1, (ii) M2 and (iii) M3. These silica gels were synthesized (a) under bulk conditions (yielding domain sizes of respectively 0.8, 3.2 and 7.0 μm) and inside micro-pillar array columns with an inter-pillar distance of (b) 7.6, (c) 5.6 and (d) 3.6 μm.

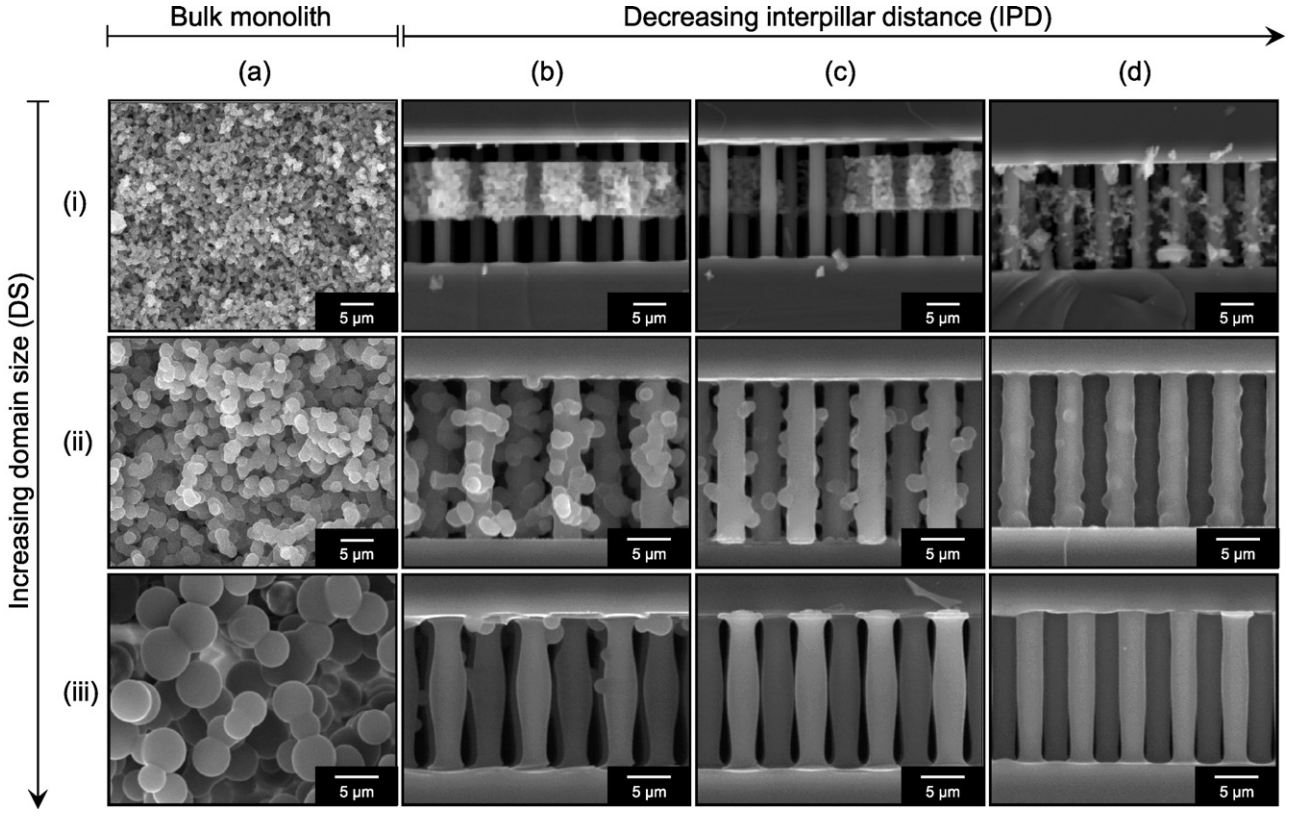

Fig. 4. SEM-images of TMOS-based gel structures, derived from three different compositions: (i) T1, (ii) T2 and (iii) T3. These silica gels were synthesized (a) under bulk conditions (yielding domain sizes of respectively 2.7, 5.5 and 8.3 μm) and inside micro-pillar array columns with an inter-pillar distance of (b) 7.6, (c) 5.6 and (d) 3.6 μm.

however when the DS/IPD ratio becomes higher than unity as is the case in Fig. 3iii-c. Eventually, when DS/IPD»1, the interconnections disappear completely and only a wetting layer on the pillar surfaces remains (Fig. 3iii-d). In this case, the long period of surface directed spinodal decomposition, combined with the relatively small distances between the pillars (i.e., a very confined space), enables the phase separation to proceed towards its energetically most favorable configuration, being the complete wetting of the pillar surface.

3.3. TMOS-based monolith synthesis in a micro-pillar array column

A major drawback in the use of MTMS-based monoliths is the lack of mesopores, hence limiting their mass loadability and retentive capacity. The experimental series discussed in Section 3.2 has therefore also been repeated using a polymerization solution with TMOS as the monomer, because it is known from literature that the resulting TMOS-based silica monoliths can be made mesoporous by heat treatment with a basic aqueous solution [35]. A drawback of the TMOS-based monoliths is that they tend to shrink strongly upon drying.

For a TMOS-based monolith, the onset of phase separation can be regulated by changing the amount of PEG (a strong hydrogen-bonding additive) in the polymerization solution. The presence of PEG reduces the tendency of the system to phase separate. Consequently, an increased amount of PEG results in smaller domain sizes by reducing the time for phase separation compared to the moment of sol–gel transition.

Different TMOS-based silica gels with increasing domain size (by reducing the amount of PEG) were synthesized in the micro-pillar array. The SEM-images of the corresponding bulk monolith are shown in the first column of Fig. 4. As can be seen in the first row of Fig. 4, the presence of micro-pillars did not affect the monolithic structure when a relatively large amount of PEG was added, yielding a small domain size compared to the inter-pillar distances (DS/IPD $\ll 1$). Unfortunately, also its tendency to shrink, which is characteristic for this type of monolith, was not altered (Fig. 4i-b and -c), except for the smallest inter-pillar distance (Fig. 4i-d) where a small reduction of the shrinkage effect can be observed. The second row of Fig. 4 shows the obtained structures when the DS/IPD ratio is increased towards unity by an increment of the monolithic domain size. In both cases where DS/IPD$\sim$1 (Fig. 4ii-b) and DS/IPD > 1 (Fig. 4ii-c and -d), the monolithic structure is completely absent and only a thick wetting layer remains on the micro-pillar surface. As can be noticed from the transition from Fig. 4 ii-b–d, this wetting layer becomes more uniform when the domain size becomes larger compared to the inter-pillar distance.

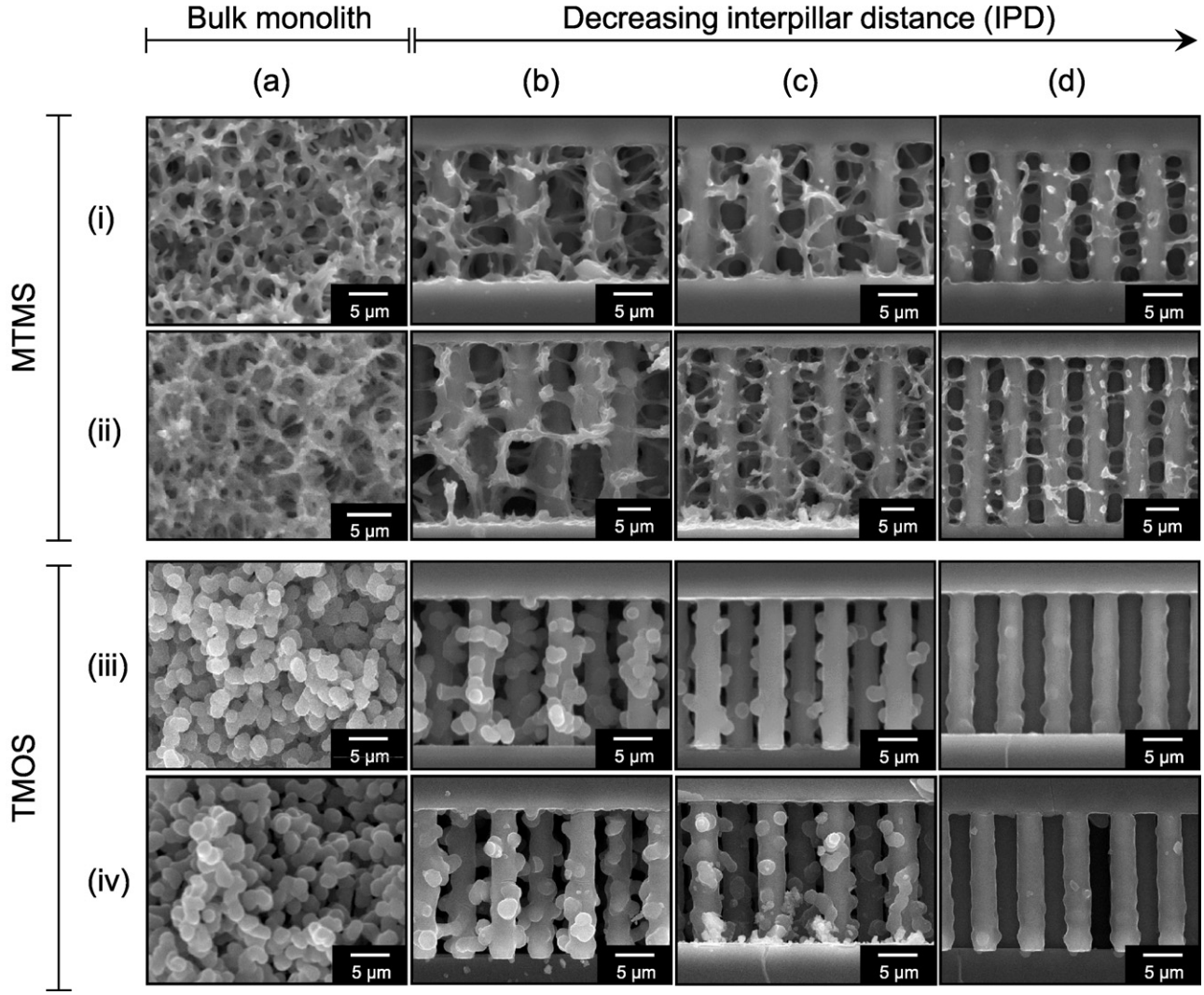

Fig. 5. SEM-images of the monolithic structures obtained for two synthesis repeats conducted with (i and ii) mixture M2 and (iii and iv) mixture T2. The symbols (a–d) have a similar meaning as in Figs. 3 and 4. The same analysis was also conducted for the other conditions (data not shown), leading to a similar degree of repeatability.

When the domain size is several times larger than the inter-pillar distance (as seen in Fig. 4iii-b–d), i.e., when the time for phase separation is very long, the uniform wetting layer displays a small, yet significant curvature. This curvature is most likely caused by Plateau-Rayleigh instability [36] of the wetting layer around the pillar, whereby the interfacial area between the gel-phase and the solvent phase is reduced, hence leading to an energetically more stable configuration.

3.4. Repeatability study

When the silica monolith syntheses were repeated under identical conditions, a good morphological repeatability could be obtained for both the MTMS-based gels and the TMOS-based gels, as illustrated in Fig. 5. Similar observations were made for the other compositions of Tables 1 and 2 (data not shown).

3.5. Implications for the preparation of chromatographic supports

The systematic variation of DS and IPD in the present study has lead to two interesting chromatographic support structures. First of all, a 3D network of linear interconnections between the micro-pillars is formed in the MTMS-based system when DS/IPD∼1 (as in Fig. 3ii-d and iii-b). In this structure, the through-pores are defined by a combination of the ordered array of micro-pillars and the linear interconnections running perpendicular to those pillars, hence leaving a monolithic structure with an improved homogeneity when compared to the monolithic structure in bulk (where pores are more randomly positioned). The obtained through-pore size of the present structures is however fairly large to be used in chromatographic columns. Future work should hence focus on the use of micro-pillar array columns with smaller inter-pillar distances. Another drawback of the MTMS-based 3D network is the lack of mesopores. This reduces the mass loadability and retentive capacity of this potential chromatographic support. TMOS-based monoliths on the other hand can be made mesoporous and a structure synthesized with this material would be preferential. Unfortunately, no similar 3D structure is observed for the TMOS-systems considered in the present study. Using TMOS, a small increase in domain size and hence time between the onset of phase separation and the sol–gel transition already causes a tremendous shift from almost no wetting to a complete wetting of the micro-pillar surface under the investigated conditions. This fast transition is however expected to be tunable by increasing the viscosity of the polymerization solution (hence, reducing the wetting velocity) or by an increment of the temperature to accelerate the phase separation and to freeze the phase separation in an intermediate stage, yielding similar homogeneous structures as those observed for the MTMS-based system.

A second interesting chromatographic support structure follows from the possibility to deposit a uniform silica wetting layer on the mantle surface of the micro-pillars when the DS/IPD-ratio is increased well above unity. Making this layer mesoporous, a mesoporous shell micro-pillar array column would be obtained with a retention surface which is several hundred times larger than the non-porous micro-pillar array columns, described in [19,20]. In contrast to the approaches previously used to increase the retention surface of micro-pillar arrays [21–23], this mesoporous layer would be deposited on both the top and bottom surface of the micro-channel, hence preventing additional band broadening by an asymmetry of mesoporosity inside the chromatographic column. Again, the size of the through-pores should be further reduced to improve the chromatographic performance of the columns. This could be realized by further reducing the inter-pillar distance, something that will be pursued in a future study with a new design of the micro-pillar array.

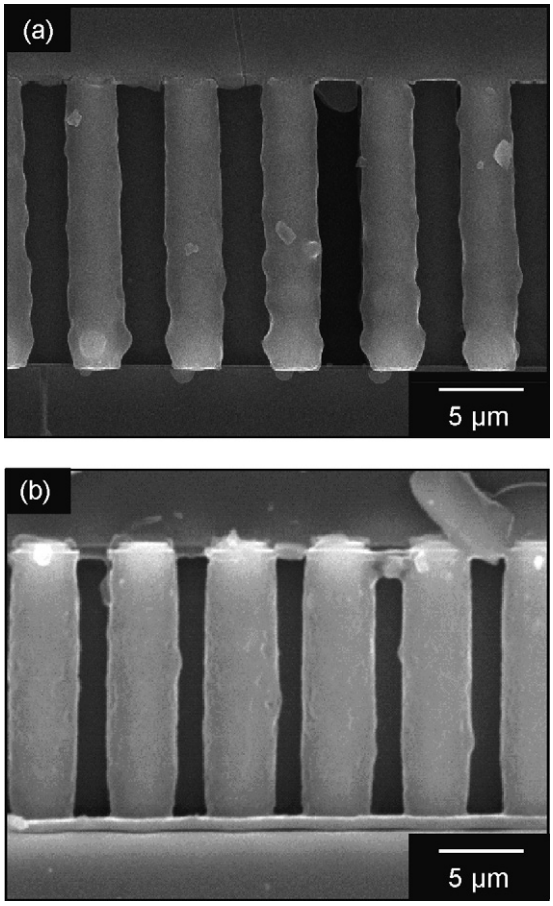

Fig. 6. SEM-images of a micro-pillar array column (IPD = 3.6 μm) (a) with one TMOS layer (composition T2) and (b) with a second TMOS layer (also using a sol–gel process with composition T2) deposited on top of the first layer.

In the present study, we followed an alternative approach and tried to reduce the through-pore size by depositing multiple layers of TMOS-material on the micro-pillar surface, by performing a sequence of two identical monolithic synthesis steps inside the same micro-pillar array channel. As illustrated in Fig. 6, an increment of the TMOS-layer thickness can be observed when two layers of TMOS-material are deposited on top of the micro-pillar surfaces, hence reducing the inter-pillar space. At the same time also the phase ratio is increased, which in turn further improves the attainable retentive capacity. A comparison between the thickness of the non-coated pillars (2.4 μm, picture not shown) and the pillar thickness after depositing one TMOS-layer reveals that the layer thickness in Fig. 6a is about 0.5 μm. With a thickness increase of about 1.0 μm between the pillars in Fig. 6a and those in Fig. 6b, the layer added during the second coating can be estimated to be about 0.5 μm, i.e., about as thick as in the first coating step.

4. Conclusion

We investigated the possibility to improve the homogeneity of sol–gel-based silica monolithic stationary phase supports by synthesizing them in the presence of an ordered array of micro-pillars. These micro-pillars act as a confined space which can influence the whole monolithic structure depending on the ratio between the monolithic domain size in bulk (quantifying the time between phase separation and sol–gel transition) and the dimension of the confined space (inter-pillar distance in the present case). The following general rules could be established.

When the domain size of the monolith is much smaller than the inter-pillar distance (DS/IPD $\ll 1$), no effect is of the presence of the micro-pillars on the monolithic structure is observed. However, when the ratio between the domain size and the inter-pillar distance approaches unity (DS/IPD$\sim$1) or rises above unity (DS/IPD > 1), the presence of the micro-pillars largely affects the monolithic structure by surface-directed phase separation. In this case, two potentially interesting chromatographic support structures are obtained. Targeting for a DS/IPD-ratio around unity, a 3D network is obtained wherein the skeleton branches are exclusively oriented perpendicular to the micro-pillar surface. The through-pore space in this structure appears more homogeneous when compared to the bulk monolith, although future work, focused on reducing the size of the through-pores, is needed before the obtained structures can be expected to give a good chromatographic performance. Increasing the DS/IPD-ratio well above unity, a second very promising chromatographic support is obtained, because in this case the micro-pillars become uniformly coated with a thick mesoporous shell. If desired the thickness of this layer can be increased by repeating the process to double the coating layer thickness.

All the observations made in this study are in full agreement with the previously reported mechanisms of monolith synthesis in confined spaces. As the underlying processes are already well documented, a further progress towards the fabrication of monolithic structures with a highly ordered configuration and optimized for chromatographic applications should be possible.

Acknowledgments

F.D. and H.E. gratefully acknowledge a research grant from the Research Foundation, Flanders (FWO Vlaanderen).

References

[1] H. Minakuchi, K. Nakanishi, N. Soga, N. Ishizuka, N. Tanaka, Anal. Chem. 68 (1996) 3498.
[2] H. Minakuchi, K. Nakanishi, N. Soga, N. Ishizuka, N. Tanaka, J. Chromatogr. A 797 (1998) 121.
[3] N. Tanaka, H. Kobayashi, K. Nakanishi, H. Minakuchi, N. Ishizuka, Anal. Chem. 73 (2001) 420A.
[4] N. Tanaka, H. Kobayashi, N. Ishizuka, H. Minakuchi, K. Nakanishi, K. Hosoya, T. Ikegami, J. Chromatogr. A 965 (2002) 35.
[5] K. Miyamoto, T. Hara, H. Kobayashi, H. Morisaka, D. Tokuda, K. Horie, K. Koduki, S. Makino, O. Núñez, C. Yang, T. Kawabe, T. Ikegami, H. Takubo, Y. Ishihama, N. Tanaka, Anal. Chem. 80 (2008) 8741.
[6] J. Billen, P. Gzil, G.V. Baron, G. Desmet, J. Chromatogr. A 1077 (2005) 28.
[7] J. Billen, P. Gzil, G. Desmet, Anal. Chem. 78 (2006) 6191.
[8] T. Hara, H. Kobayashi, T. Ikegami, K. Nakanishi, N. Tanaka, Anal. Chem. 78 (2006) 7632.
[9] S. Altmaier, K. Cabrera, J. Sep. Sci. 31 (2008) 2551.
[10] P. Gzil, J. De Smet, G. Desmet, J. Sep. Sci. 29 (2006) 1675.
[11] B. He, N. Tait, F.E. Regnier, Anal. Chem. 70 (1998) 3790.
[12] F.E. Regnier, J. High Resolut. Chromatogr. 23 (2000) 19.
[13] B.E. Slentz, N.A. Penner, F.E. Regnier, J. Sep. Sci. 25 (2002) 1011.
[14] P. Gzil, N. Vervoort, G.V. Baron, G. Desmet, Anal. Chem. 75 (2003) 6244.
[15] P. Gzil, J. De Smet, N. Vervoort, H. Verelst, G.V. Baron, G. Desmet, J. Chromatogr. A 1030 (2004) 53.
[16] J. De Smet, P. Gzil, N. Vervoort, H. Verelst, G.V. Baron, G. Desmet, Anal. Chem. 76 (2004) 3716.
[17] M. De Pra, W.Th. Kok, J.G.E. Gardeniers, G. Desmet, S. Eeltink, J.W. van Nieuwkasteele, P.J. Schoenmakers, Anal. Chem. 78 (2006) 6519.
[18] M. De Pra, W. De Malsche, G. Desmet, P.J. Schoenmakers, W.T. Kok, J. Sep. Sci. 60 (2007) 1453.
[19] W. De Malsche, H. Eghbali, D. Clicq, J. Vangelooven, H. Gardeniers, G. Desmet, Anal. Chem. 79 (2007) 5915.
[20] H. Eghbali, W. De Malsche, J. De Smet, J. Billen, M. De Pra, W.Th. Kok, P.J. Schoenmakers, H. Gardeniers, G. Desmet, J. Sep. Sci. 30 (2007) 2605.
[21] W. De Malsche, D. Clicq, V. Verdoold, P. Gzil, G. Desmet, H. Gardeniers, Lab Chip 7 (2007) 1705.
[22] W. De Malsche, H. Gardeniers, G. Desmet, Anal. Chem. 80 (2008) 5391.
[23] A. Fonverne, F. Ricoul, C. Demesmay, C. Delattre, A. Fournier, J. Dijon, F. Vinet, Sens. Actuators B: Chem. 129 (2008) 510.
[24] D. Allen, Z. El Rassi, Electrophoresis 24 (2003) 3962.
[25] A.-M. Siouffi, J. Chromatogr. A 1000 (2003) 801.
[26] K. Nakanishi, Bull. Chem. Soc. Jpn. 79 (2006) 673.
[27] G. Guiochon, J. Chromatogr. A 1168 (2007) 101.
[28] K. Kanamori, K. Nakanishi, K. Hirao, H. Jinnai, J. Sol-Gel Sci. Technol. 26 (2003) 157.
[29] K. Kanamori, K. Nakanishi, K. Hirao, H. Jinnai, Colloid Surf. A: Physicochem. Eng. Aspects 241 (2004) 215.
[30] K. Kanamori, H. Yonezawa, K. Nakanishi, K. Hirao, H. Jinnai, J. Sep. Sci. 27 (2004) 874.
[31] K. Kanamori, K. Nakanishi, K. Hirao, H. Jinnai, J. Sol-Gel Sci. Technol. 35 (2005) 183.
[32] Y. Suzumura, K. Kanamori, K. Nakanishi, K. Hirao, J. Yamamichi, J. Chromatogr. A 1119 (2006) 88.
[33] H. Tanaka, J. Phys.: Condens. Matter 13 (2001) 4637.
[34] S. Puri, J. Phys.: Condens. Matter 17 (2005) R101.
[35] K. Nakanishi, H. Shikata, N. Ishizuka, N. Koheiya, N. Soga, J. High Resolut. Chromatogr. 23 (2000) 106.
[36] P.-G. de Gennes, F. Brochard-Wyart, D. Quéré, Capillarity and Wetting Phenomena: Drops, Bubbles, Pearls, Waves, Springer, New York, 2003.